Modeling the Effect of Carburization and Quenching on the Development of Residual Stresses and Bending Fatigue Resistance of Steel Gears

Zhichao Li, Andrew M. Freborg, Bruce D. Hansen, and T.S. Srivatsan

Most steel gears are carburized and quenched prior to service to obtain the desired specific strength (σ/ρ) and hardness requirements. Use of carburization and quenching of steel gears creates a compressive residual stress on the carburized surface, which is beneficial for improving both bending and contact fatigue performance. Also, higher carbon content in the carburized surface decreases the starting temperature for formation of the martensitic phase and delaying the martensitic transformation at the part surface during the quenching hardening process. During the martensite phase formation, the material volume expands. The delayed martensitic transformation, coupled with the associated delayed volume expansion, induces residual compressive stress on the surface of the quenched part. The carburized case depth and distribution of carbon affect both the magnitude and the depth of the resulting residual compressive stress. In this article, the effect of carbon distribution on the residual stress in a spur gear is presented and discussed using finite element modeling to understand the intrinsic material mechanics contributing to the presence of internal stress. Influence of the joint on thermal gradient and the influence of phase transformation on the development of internal stresses are discussed using results obtained from modeling. The residual stress arising due to heat treatment is imported into single-tooth bending and dynamic contact stress analysis models to investigate the intrinsic interplay among carbon case depth, residual stress, bending load, and torsional load on potential fatigue life. Three carburization processes, followed by oil quenching, are examined. A method for designing minimum case depth so as to achieve beneficial residual stresses in gears subjected to bending and contact stresses is suggested.

1. Introduction

Parts made from low carbon steel are often carburized to increase both the hardness and strength of the surface, while maintaining the core in a tough and ductile condition. The carburization and quenching processes not only aids in enhancing both surface hardness and strength but also tends to introduce compressive residual stress in the carburized layer. This aid in increasing the fatigue life by counteracting the bending and contact stresses that are introduced during loading. The depth and magnitude of compressive residual stresses are readily influenced by both part geometry and depth of the

Dr. T. S. Srivatsan is a Member of Editorial Board of JMEP.

Zhichao Li and **Andrew M. Freborg**, Deformation Control Technology, Inc., 7261 Engle Road, Suite 105, Cleveland, OH 44130; **Bruce D. Hansen**, Sikorsky Aircraft Corporation, 6900 Main Street, Stratford, CT 06615; and **T.S. Srivatsan**, Division of Materials Science and Engineering, Department of Mechanical Engineering, The University of Akron, Akron, OH 44325. Contact e-mails: zli@ DeformationControl. com, Andy.freborg@deformationcontrol.com, bruce.hansen@sikorsky. com, and tsrivatsan@uakron.edu.

carburized case. A greater depth of the residual compressive stress alone does not necessarily equate to improved fatigue resistance. This is because fatigue crack initiation is primarily a surface phenomenon, and high-cycle fatigue (HCF) life is primarily controlled by crack initiation (Ref 1).

With sustained and noticeable improvements in computer hardware and modeling technology, finite element analysis (FEA) is being increasingly used in the manufacturing industry. In more recent years, engineering analysis software for heat-treatment modeling have been developed and effectively used to predict residual stresses and related distortion (Ref 2, 3). Through numerical analysis, the response of a part to: (i) thermal stress, (ii) phase transformation, and (iii) geometry can be easily understood (Ref 4-7). The knowledge gained from calibrated modeling can be put to effective use toward improving both part design and the heat-treatment process.

A deep carbon case tends to reduce the magnitude of residual compressive stress on the surface resulting from quench hardening. The reason for this will be explained in this article. During active service, the contact between the driver and the driven gears creates stresses that penetrate into the part surface. The magnitude and the depth of these contact stresses are key to understanding contact fatigue performance. For service conditions, which create deeper contact stresses, a deeper carburized case is both essential and required. The heat-treatment process is the primary means by which beneficial compressive stresses are introduced. Currently, there is limited information in the published literature quantifying the synergistic and/or mutually interactive influences of these effects.

In this article, finite element models are developed to study residual stresses arising from three vacuum carburization schedules, followed by a standard oil quench hardening process. The objective of this study is to demonstrate the compounding and controllable effects of residual stress developed during processing on the effective stress experienced under service loads. To demonstrate this concept, the residual stresses predicted from the oil quench models are imported into single-tooth bending and contact stress analysis models of a spur gear under load. The effect of (a) carburization, (b) heat-treatment residual stresses, (c) bending stresses, and (d) related contact stresses are then examined and appropriately discussed. Conclusions are then drawn concerning (i) the interaction of carburization, quenching, and gear geometry on residual stress state and (ii) their benefit in response to service stresses introduced during subsequent part loading.

2. The Finite Element Model

The geometry of the spur gear chosen for use in this study is shown in Fig. 1. The tip diameter of the gear is 95 mm, the inner diameter is 30 mm, and the gear face width is 6.35 mm. The hub thickness is 19.05 mm. The gear has a total of 28 teeth. The gear steel chosen for this study was AMS 6308 (Pyrowear®53), having a chemical composition (wt.%): 0.10 C, 0.35 Mn, 1.00 Si, 1.00 Cr, 2.00 Ni, 3.25 Mo, 2.00 Cu, and 0.10 V.

The single-tooth finite element model developed for the gear is also shown in Fig. 1. Using boundary conditions with cyclic symmetry, the single-tooth model can represent the whole gear with an assumption that all teeth experience the same conditions circumferentially during heat treatment. The single-tooth finite element model has 26,256 nodes and 22,854 hexahedral linear elements. Fine elements were used on the gear tooth surface with the primary purpose of identifying: (i)
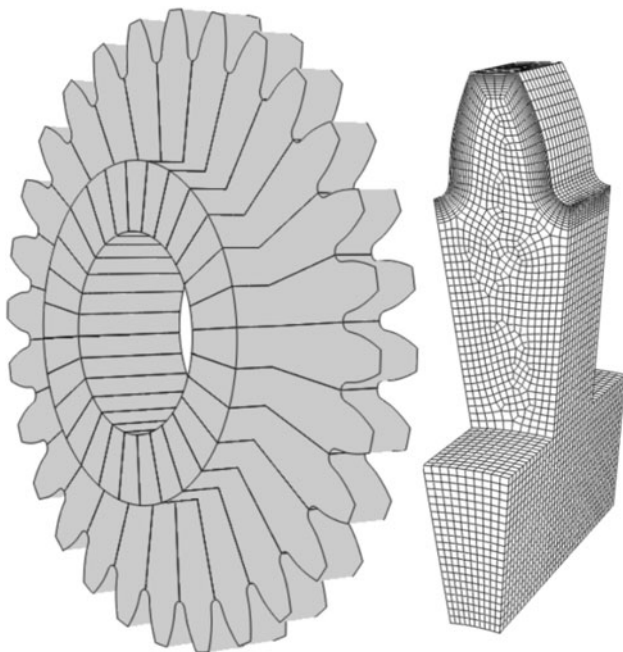
the carbon gradient and (ii) the thermal gradient during heat treatment.

3. Effect of Vacuum Carburizing Case Depth

Vacuum carburization is being increasingly used in heat treatment due to the benefits of reduced furnace time and superior as-carburized product quality. The effect of three carburized case depths on residual stress was examined using the models: 0.5, 1.0, and 1.5 mm.

For this study, case depth was defined as the distance from the outer surface to a depth having a carbon content of 0.4 wt.%. The expected carbon content on the surface is 0.8 wt.%. DANTE-VCARB software was used to design the "boost and diffuse" schedule for the vacuum carburization process to meet requirements for: (i) 0.8 wt.% carbon and (ii) the three defined case depths. Acetylene was used as the carburizing gas, with only the tooth surface being carburized to be consistent with standard aerospace gear practice. All other surfaces, to include the gear tip, were considered masked to carbon diffusion, which is typically accomplished through copper-plating during the physical processing of these parts. This is done to avoid the potential for localized areas at the tip of the teeth and any other section size changes from having excessive carbon concentrations that could result in the formation and the presence of deleterious carbides both on the surface and the interior.

The furnace processing times for the three vacuum carburization schedules are shown in Table 1. It is to be noted that individual boost times, as well as overall furnace processing times, increase with case depth. This is primarily because the carbon gradient drops significantly as diffusion from the surface occurs. To minimize the total carburization time, additional boost cycles were used to facilitate continuous diffusions.

Figure 2 shows the predicted carbon distribution for an effective case depth of 1.5 mm subsequent to vacuum carburization. The carbon content at the "root" surface is about 0.68%, which is lower than the 0.8% carbon at the tooth flank surface. This is an important illustration of how geometry does affect the "local" carburization response, which will subsequently influence the "local" quench hardening and residual stress response. A cross section through the middle thickness of the gear is shown in Fig. 3. Two directions, shown as straight lines in the cut section, can be used to examine the following effects:

(i) A comparison of carbon distribution for the three carburization schedules.
(ii) The temperature, phase, and stress evolutions during quenching.

Fig. 1 Gear geometry and finite element mesh of single tooth model

Table 1 Comparison of furnace times of three vacuum carburization schedules

Case depth	0.5 mm	1.0 mm	1.5 mm
Boost time, s	848.0	1668.0	2460.0
Diffuse time, s	3608.0	17256.0	40930.0
Furnace time, s	4456.0	18924.0	43390.0
R value	4.25	10.35	16.64
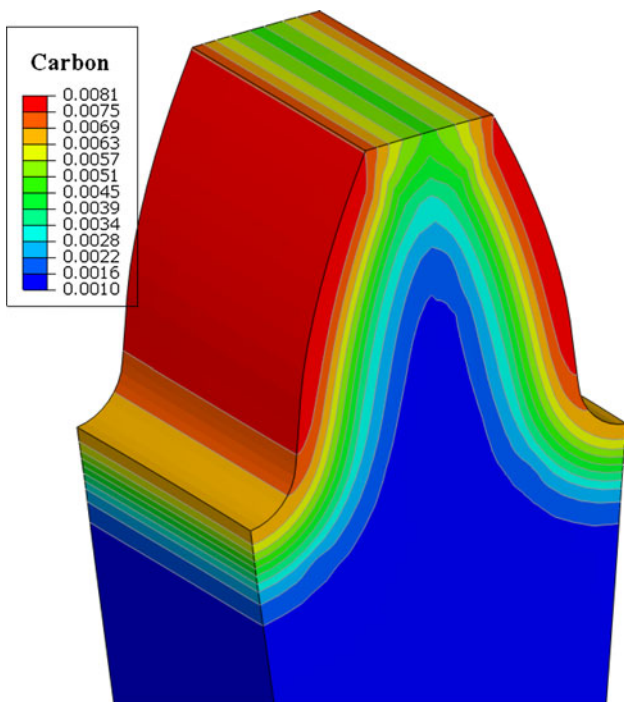
Fig. 2 Carbon distribution contour with case depth of 1.5 mm

Fig. 4 Carbon distributions in terms of depth and increased geometry effect with case depth
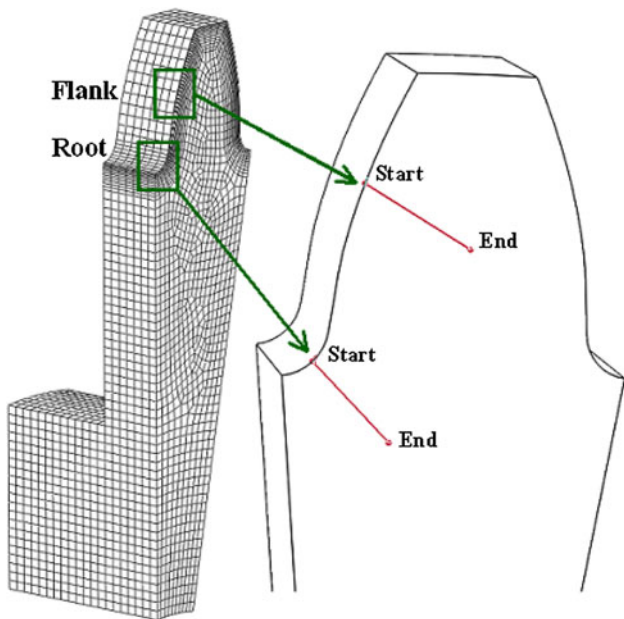

Fig. 3 Cross section and two straight lines selected for modeling result analysis

The influence of geometry on carbon distribution can be noticeably significant. With an increase in carburization time and depth of the carbon case, the effect and/or influence of geometry also increases. The gear tooth flank has a convex shape, which is close to being flat. However, the root area has significant geometric curvature, resulting in localized radial dilution of the diffusing carbon. The difference in carbon content between the flat flank and curved root increases with case depth. This is shown in Fig. 4. For the three different case
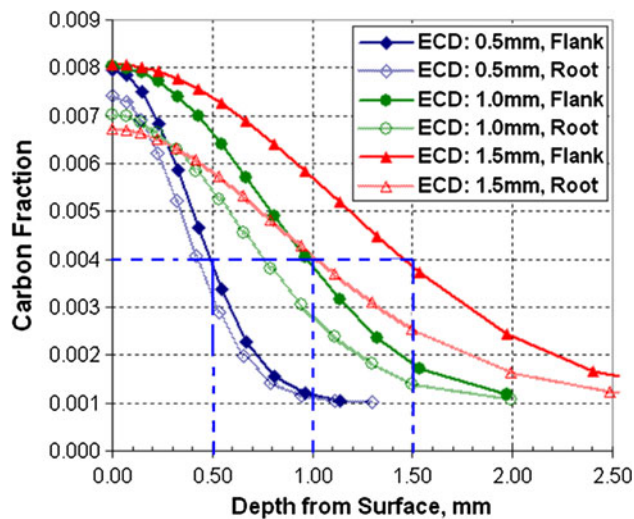
depths examined in this article, the differences in "local" carbon content between the flank and the root are 0.06% for a carburized case of 0.05 mm, 0.10% for a carburized case of 0.10 mm, and 0.13% for a carburized case of 0.15 mm. Therefore, the influence of "local" gear tooth geometry must be considered during the vacuum carburization process so as to be able to both guarantee sufficient carbon content on the surface, while concurrently ensuring case depth and the carbon content needed to promote required martensite formation and consequent residual stress formation. Furthermore, use of the one-dimensional analytical modeling approach provides a viable basis for the first step in designing the carburization process.

4. Modeling the Quenching Process

Upon carburization, the gear is (a) quench hardened in oil, (b) cryogenically treated to minimize the amount of retained austenite, and then (c) double tempered. Finite element process models for the three carburization scenarios examined previously were extended to include the quench hardening and cryogenic treatment prescribed for AMS 6308. This was done to further assess the residual stress effects arising from the geometry-induced, variable carburization response. The DANTE finite element software was used for these models. DANTE uses an internal state variable (ISV) material model, linking temperature and time-dependent phase transformation kinetics with a material mechanics (stress) model describing both temperature and material strain rate dependencies (Ref 8) The software provides accurate predictions of microstructural, residual stress, and distortion response, and is especially useful in evaluating process sensitivities by facilitating an examination of the in situ material response during heat-treatment processing.

The minimum principal residual stresses predicted for each condition following cryogenic treatment are shown in Fig. 5. The carburized tooth surface shows compressive residual stresses, with depth of compressive stress increasing with increasing case depth. The magnitude of residual compressive stress in the fillet area of the root is noticeably higher than that
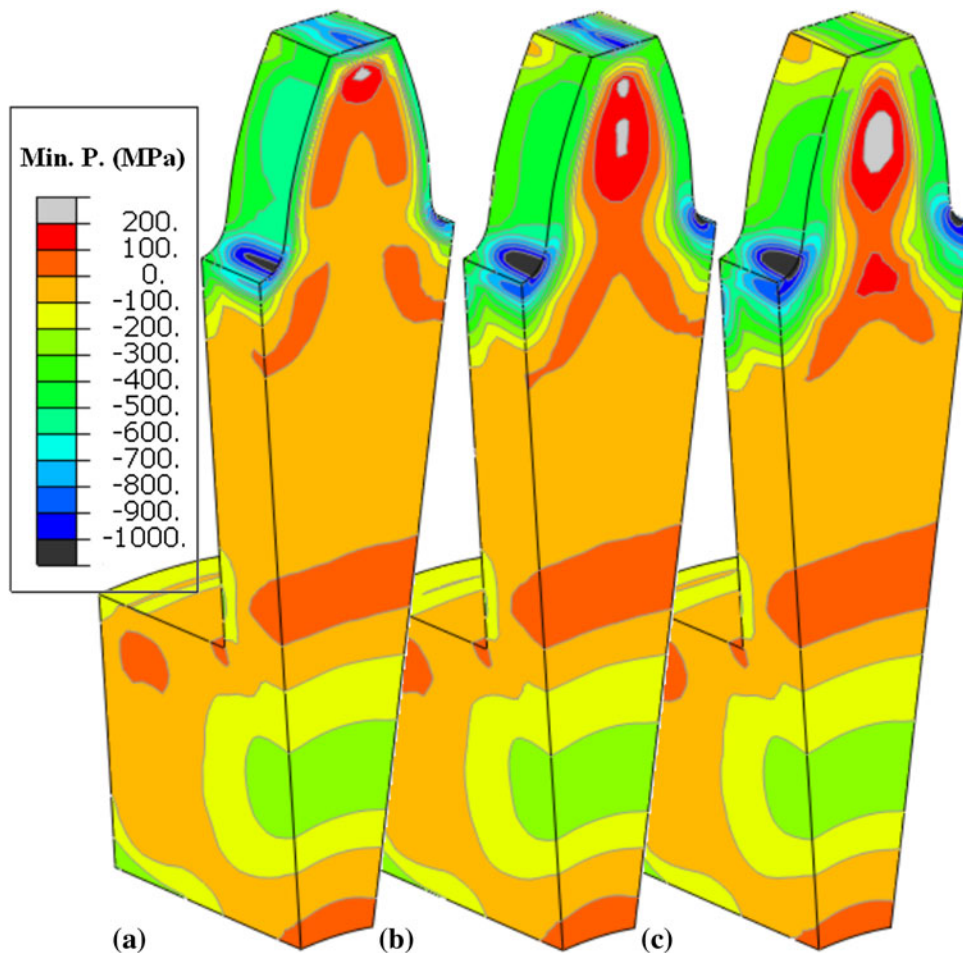
Fig. 5 Cut view of residual stress distributions for three carbon cases. (a) 0.5 mm, (b) 1.0 mm, and (c) 1.5 mm

in the flank area of the root. This can be ascribed to be due to the geometry effect.

4.1 Stress Evolution During Quenching

Dilatometry experiments were conducted with the primary purpose of characterizing the phase transformation kinetics of AMS6307 alloy steel for use in process modeling. No diffusive phases (i.e., ferrite, pearlite, or bainite) were observed to form during cooling (Ref 8). The only second-phase microconstituent present in the microstructure subsequent to quenching is martensite.

The martensite transformation start temperature (M_s) decreases with an increase in carbon content. The M_s for AMS 6307 having 0.1 wt.% carbon is 437 °C; while the M_s of the same steel carburized to 0.8 wt.% carbon is 135 °C. With this surface carbon gradient, the martensite phase transformation during oil quenching starts from under the surface at the case-core interface, even though the temperature at the surface is significantly lower than the temperature in the interior. Also, there is a volumetric expansion associated with martensite transformation. The delayed transformation of the carburized case relative to interior of the gear results in compressive residual stresses on the surface, as shown in Fig. 5. For a deeper carbon case, the residual compressive stresses will be deeper. It should also be noted that for all the three case depths

examined, the root fillet region reveals a higher residual compressive stress than the adjacent flank region.

Evolution of residual stress development during oil quench is shown in Fig. 6 for both the gear flank and root fillet regions, using the gear carburized to a case depth of 1.0 mm as the basis. Stress evolution in the alloy steel gear during quenching is a combination of thermal, phase transformation, and geometry effects. The process modeled for this study was furnace re-heating of the carburized and cooled gear to 900 °C, a 10 s transfer through air to the quench station, and subsequent immersion and holding in agitated oil.

During the early stages of quenching prior to the initiation of phase transformation, the thermal shrinkage on the surface creates a tensile stress on the surface. Upon further cooling, the martensitic transformation starts immediately below the carburized surface, at the case-core interface, when the temperature drops below the local M_s. A compressive stress is then generated immediately below the surface by this phase transformation. To balance the sub-surface compressive stresses, the surface with high carbon content goes into tension.

At this point, the high carbon content on the surface is still austenitic and has a low yield stress relative to the transformed subsurface material. Tensile stresses on the surface are conducive for plastic deformation. Upon further cooling, the phase transformation front moves toward the gear tooth surface. The high carbon content surface finally transforms to martensite, as
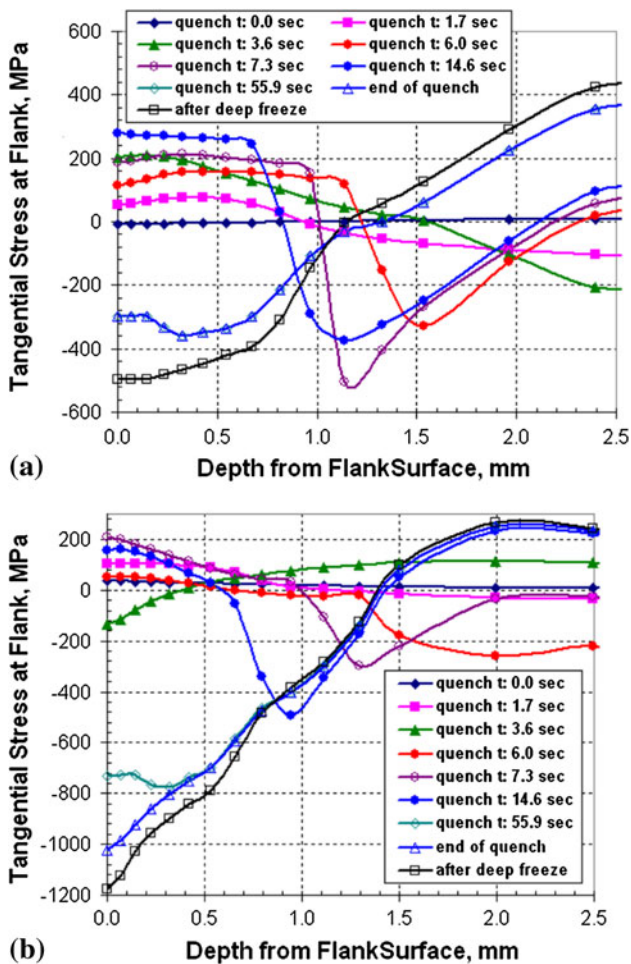
Fig. 6 Stress evolution due to thermal gradient and phase transformation (a) gear flank and (b) root fillet

shown in Fig. 6(a), the surface has a compressive residual stress at the end of the oil quench. However, at 0.8 wt.% carbon, the surface of the AMS 6307 gear has a martensite finish temperature (M_f) lower than the oil temperature. This typically results in 20-25% retained austenite for the carburized alloy subsequent to oil quenching. AMS 6307 is therefore typically cryogenically treated following quenching to reduce the retained austenite content to below 3%. During cryogenic treatment, the additional martensite formation that occurs on the carburized surface will tend to further increase the magnitude of compressive stress on the surface.

The variation of in-process stress evolution in the gear flank and root fillet is shown in Fig. 6(a) and (b), respectively. Differences in stress distribution arise mainly from geometry. The gear flank has a relatively flat surface, and its response to quenching is quite similar to that experienced by a simple cylinder. Response of the alloy steel to both thermal gradient and phase transformation is primarily one-dimensional at this location. In contrast, the root fillet region shows a higher concentration of stress caused by the local radius. The residual compressive stress at the root fillet region is over 1000 MPa, which is significantly higher than that of the gear flank.

Both the thermal gradient and the phase transformation also contribute to "local" stress concentration at and around the root fillet region during quenching. The temperature of the gear flank is noticeably lower than temperature of the gear root and

fillet regions during the entire quenching process primarily because of local surface area to mass differences. The cooling rate experienced by the gear flank is much higher during the early stages of quenching. The cooling rate at the gear root gradually catches up and even exceeds the cooling rate at the gear flank as the cooling gradually progresses. The observed non-uniform cooling arising from gear geometry contributes to the presence of "local" stress concentration in the fillet.

A third factor contributing to the presence of stress concentration in the root fillet is phase transformation. The martensite and stress distributions in the gear following 3.6 s into the quench process are shown in Fig. 7(a) and (b), respectively. The stress contour map reveals the stresses to be tangential to the gear tooth surface. Figure 7(a) shows the martensite formation to initiate under the high carbon surface. The volume expansion occurring at the core of the tooth generates about 300 MPa of compressive stress at this stage, as shown in Fig. 7(b). To balance the compressive stress, the gear flank responds with a stress of 200 MPa in tension. Interestingly, the volume expansion of the gear tooth creates a bending effect around the region of the root fillet, thereby placing the fillet region under compression. This is the key factor, which causes a significant difference in the residual stress between the gear flank and the root fillet, as shown previously in Fig. 6(a) and (b), respectively.

The response of the material at the gear flank during quenching is similar to that experienced by a generalized cylindrical part. To illustrate this point, Fig. 8(a) shows the tangential residual stresses as a function of depth from the flank surface, for all the three examined carburization scenarios. The models reveal the depth of residual compressive stress to increase with depth of the carbon case. However, magnitude of the residual compressive stress on the surface decreases with depth of the carbon case. The predicted tangential residual compressive stresses at the surface of the gear flank for case depths of 0.5, 1.0, and 1.5 mm are 570, 500, and 400 MPa, respectively. Such a response may not be intuitively obvious to steel heat-treating processors. The results from the DANTE process models provide a reasonable explanation for this effect primarily because they illustrate the evolution history corresponding to the distribution of carbon for each carburizing depth.

Figure 8(b) shows the tangential residual stresses plotted in terms of depth from the root fillet surface. Here, a greater depth of carbon increases both the magnitude and the depth of the residual compressive stresses. However, the residual stress difference between case depths of 0.5 and 1.0 mm is noticeably more than the residual stress difference between case depths of 1.0 and 1.5 mm. Also, the carburization furnace time of a 1.5 mm case depth is 2.3 times more than that of a 1.0 mm case depth, as shown in Table 1. Selection of case depth of carbon should be, therefore, based on both cost considerations and service loading conditions experienced by the gear.

5. Gear Loading Models

The ultimate importance of residual stresses lies in their ability to either mitigate or exacerbate stresses induced in the part from service loads. To evaluate the composite effects of residual and loading stresses on the test gear, the quenching stresses predicted from heat-treatment models were imported
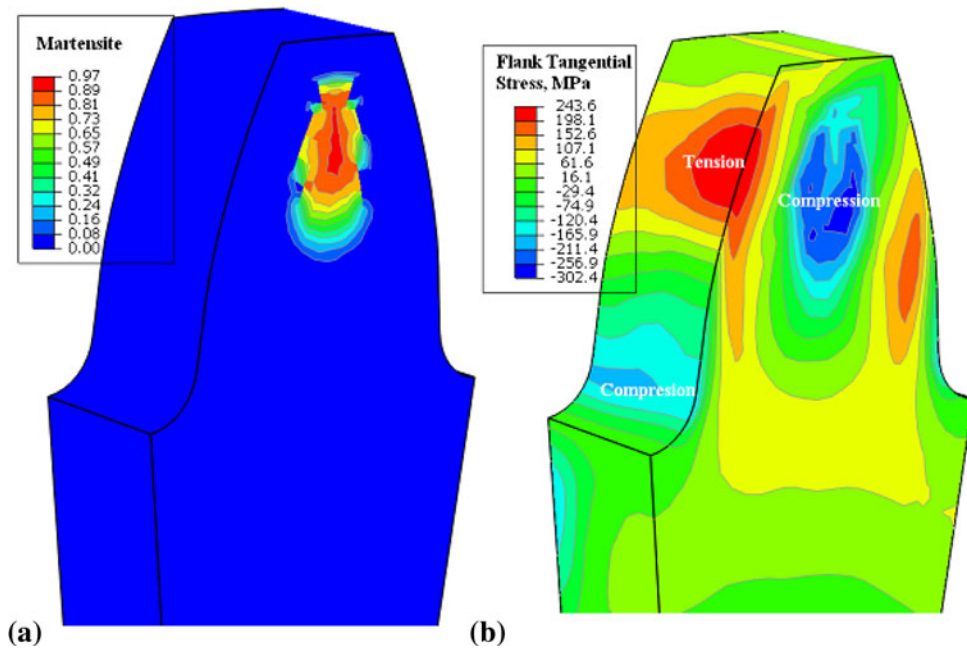
Fig. 7 Cut view of (a) martensite distribution and (b) stress distribution, at 3.6 s during quench using the 1.0 mm effective case depth study
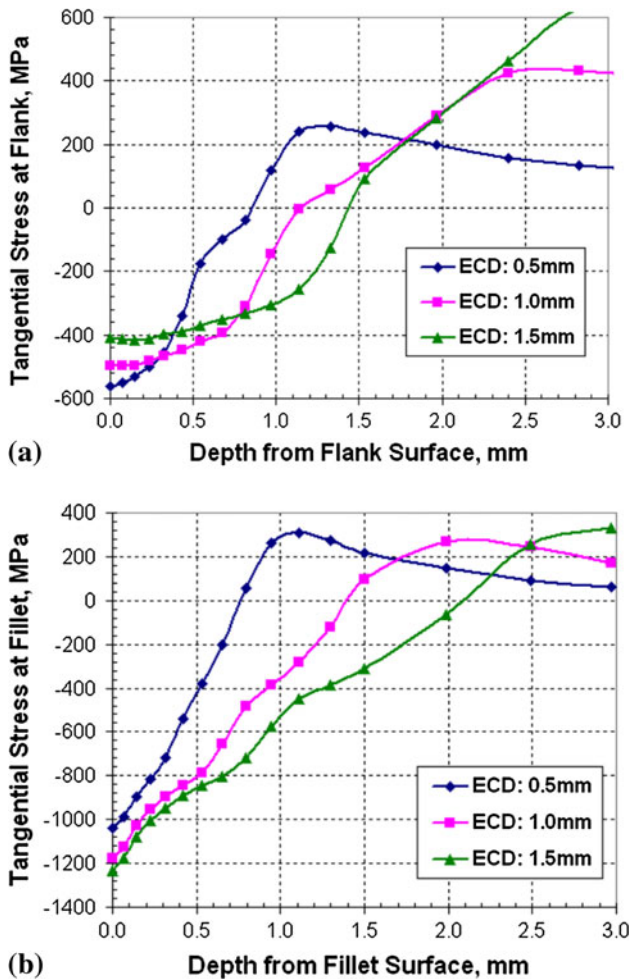

Fig. 8 Predicted residual stresses in terms of depth from three carburization case depths at (a) root fillet and (b) gear flank regions

into single-tooth bending and dynamic contact models. To determine the specific influence of residual stress, loading models without heat-treatment residual stress were concurrently evaluated to understand the significance of the heat-treatment process on loading response.

5.1 Single-Tooth Bending Load Model

As described, the spur gear used in this study had 28 teeth. The single-tooth bending load model included all 28 teeth, using the single-tooth DANTE heat-treatment model as a basis and using cyclic symmetry to build the full gear. The residual stresses from the heat-treatment model with the 1.0 mm carburized case were mapped into the 28 teeth of the bending model. A bending load was then applied to an area close to the tooth tip, as shown in Fig. 9(a). The maximum applied force in the bending fatigue experiment was 11,250 Newton's (2925 lbf), with the resulting stress distribution contour for the loaded and heat-treated gear shown in Fig. 9(a). The stresses plotted in Fig. 9(a) are the radial stresses, which are (a) close to the tangential direction along the regions of both the root fillet and gear flank and (b) close in magnitude to the maximum principal stress in these areas. The tensile stress in the root fillet region is about 980 MPa. The opposite root fillet is under compressive stress, having a magnitude of about 1800 MPa. Increasing the bending load causes the highest stress location at the root fillet to move away from the root and toward the tooth tip along the gear flank.

By taking the residual stresses arising from the quenching process for the three carbon case depths and applying the maximum bending load, one can safely estimate the stresses in the root fillet. The stresses in the root fillet region are plotted as a function of depth from the root fillet surface and shown in Fig. 9(b). A bending model was also conducted without including the heat-treatment residual stresses, and is also shown in Fig. 9(b). The tensile stress on the surface under
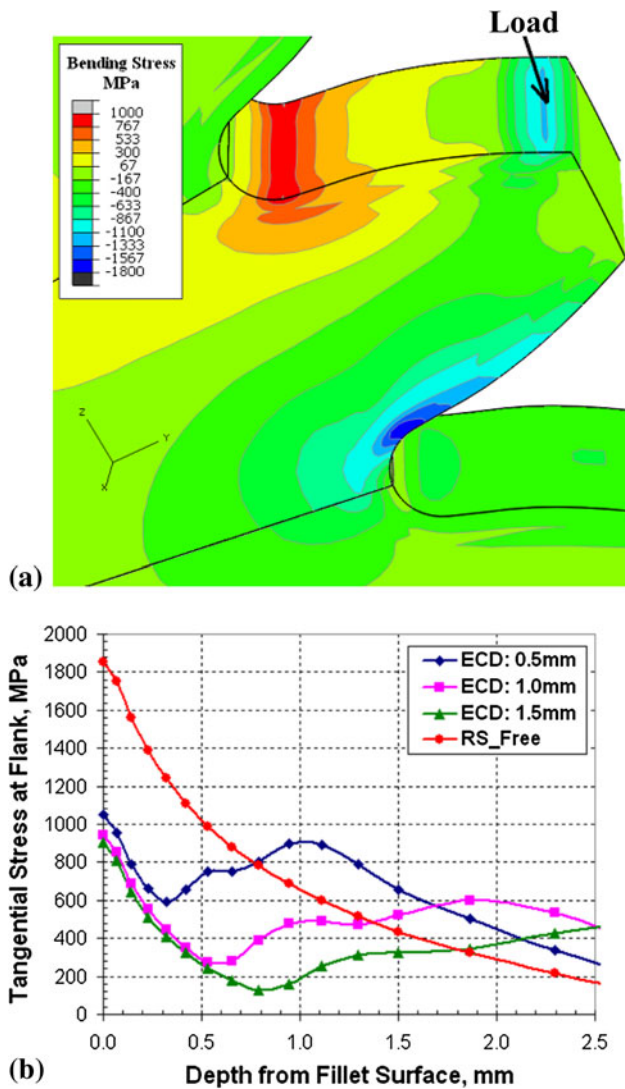
Fig. 9 Single-tooth bending stress distribution. (a) Contour plot for 1.0 mm carbon case depth and (b) stress distribution in terms of depth

bending is about 1800 MPa, which is close to the yield stress of high carbon tempered martensite. By adding the residual compressive stress arising due to carburization and quenching, the effective tensile stresses at the root fillet drop to 1000 MPa under the influence of a bending load. Therefore, the residual compressive stresses can have an important influence on the magnitude of effective stress experienced locally by a gear in service.

Linear elastic material properties were assumed for the loading models, and the yield stress for the gear steel is assumed to be 1800 MPa with hardening. Furthermore, it is assumed that single-tooth bending is a geometrically and materially linear problem below material yielding. By adding the heat-treatment residual stresses and pure bending stresses, the combined stress matches with the predicted stress distribution, as shown in Fig. 9(b). These comparisons clearly reveal the residual stress from heat treatment to be critical to the bending fatigue performance of the gear.

The influence of depth of residual compressive stress on single-tooth bending fatigue performance is not conclusive

(Ref 9). There is as yet no proof that a 0.5 mm carbon case would have an inferior bending fatigue performance when compared with the other two cases.

5.2 Dynamic Contact Stress Analysis

Finally, contact stress analyses were conducted using gears that were initially stress free or gears that contained the residual stress state due to quench hardening. This was done to illustrate the effect of residual stress on contact fatigue performance. The applied torque was adjusted such that the effect of bending on the root fillet region matched the maximum single-tooth bending load. The torque applied in this model was noticeably higher than the torque typical of service conditions. However, this exercise was done with the objective of understanding the effects of heat-treatment processing on carburized case depth. The same material properties were used in this model as in the case of the single-tooth bending model(s).

The contact Mises stresses, without the effects of heat-treatment residual stresses is shown in Fig. 10(a). The highest contact stress occurs immediately below the contact surface, and plastic deformation is predicted to occur. In this case, the gear would be expected to experience a low contact fatigue life, and fail by spalling. However, with the residual stresses from heat treatment, the combined stresses under the contact surface are reduced, as shown in Fig. 10(b).

Mises stress distributions along line are plotted in Fig. 11 for several different case depths. The Mises stress requires definition of orientation, and in Fig. 11 the X-axis represents the distance from surface point A, where $X = 0.0$. The left Y-axis is the Mises stress, and the right Y-axis is the carbon content in weight fraction. The curve with solid triangle marks represents the contact stresses without the heat-treatment residual stresses. Plastic deformation is shown between the depths of 0.20 and 0.55 mm by the plateau of the curve with stress values of about 1800 MPa. A high strength material is required deeper than 0.5 mm, so that the carburized case can extend deeper than 0.5 mm. The Mises stress on the surface drops from 950 to 625 MPa. The highest stress occurs at a depth of 0.4 mm, having a stress magnitude of about 1500 MPa, which is reduced significantly from the condition without considering the heat-treatment residual stresses.

Both the material's strength and the quenching residual stresses in the region of high contact stresses should be considered to realize improved contact fatigue behavior of the gear. As mentioned in a previous section, a deeper carbon case does not necessarily produce a higher magnitude of residual compression. The magnitude of the residual compression at the gear flank region is higher for the 1.0 mm carbon depth than that of 1.5 mm carbon between the flank surfaces to a depth of 0.75 mm. A carbon case deeper than 1.0 mm does not contribute to contact fatigue behavior. As shown by the shaded area in Fig. 11, a carburization case depth between 0.75 and 1.0 mm is preferred for a combination of bending fatigue and contact fatigue behavior, as also reduced carburization cost.

6. Conclusions

Investigation of the effects of geometry and heat-treating process variables on residual stress and effective stress
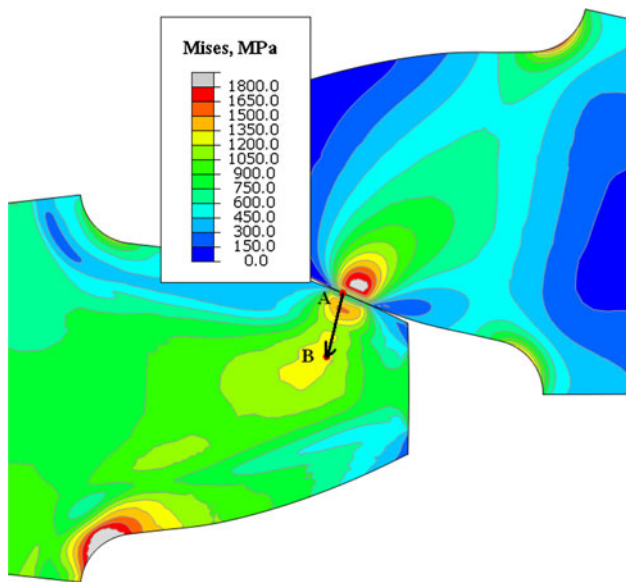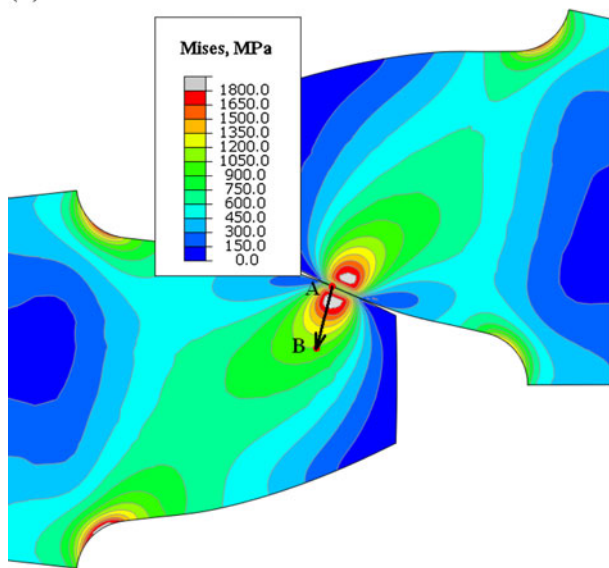
Fig. 10 Stress distributions from the dynamic contact analyses. (a) Without heat-treatment residual stresses and (b) with heat treatment residual stresses in one tooth

encountered in bending and dynamic service loads revealed the following:

1. Process simulation of the vacuum carburizing process with the DANTE VCARB mass diffusion model showed that gear tooth geometry affects local carbon distribution by dispersing carbon more widely in the gear root. This reduces the local carbon content, resulting in a higher local martensite formation temperature. The change in martensite formation timing in turn affects residual stress by reducing the magnitude of the final residual compression.
2. For this spur gear, the residual compressive stresses from quench hardening are greatest in the gear tooth fillet area.
3. Carburization increases the magnitude of surface compression achieved from quench hardening by delaying the surface martensitic transformation.
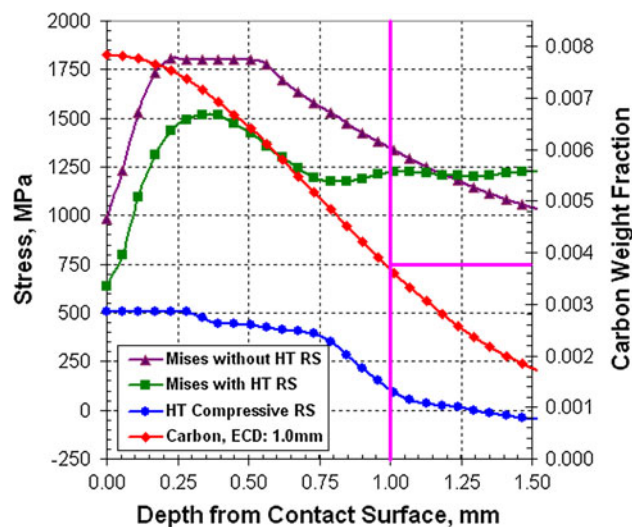

Fig. 11 Relation between contact stresses and design of carbon case depth

4. Process simulation shows that residual stress evolution is affected by geometry, local thermal gradients, and the surface carbon profile. All act to increase local compressive residual stresses from carburization and quench hardening of gear geometries.
5. The depth of residual compressive stresses increase with depth of the carburized case.
6. The magnitude of the surface residual compression decreases nonlinearly with increased case depth. Maximum case depth examined in this study was 1.5 mm.
7. Single-tooth bending load models show surface tension from loading to be decreased by the presence of surface residual compression. Theoretically, this should reduce the driving force for crack initiation in HCF. Failure in HCF is principally dominated by crack initiation as opposed to propagation. Thus, decreasing the crack initiation driving force by increasing the stresses required to initiating a crack will theoretically increase the endurance limit in HCF.
8. Residual surface compression from carburization and quench hardening also reduces the effect of contact stresses during gear tooth dynamic loading.
9. Deeper carburized case depth with associated deeper residual compression does not necessarily decrease dynamic loading effective stress. Gear geometry and heat-treatment response determine the optimal depth of compression. For this spur gear, an ECD of 0.7 mm appears to be the optimum ECD and deeper ECD's offer no further benefit.
10. Process simulation represents an important analytical tool to investigate the compounding effects of process, material, and part geometry influences on residual stress response from heat treatment, and subsequent part response from service loads.

References

1. S. Suresh, *Fatigue of Materials*, Cambridge University Press, Cambridge, 1998
2. B. Ferguson and W. Dowling, *Predictive Model and Methodology for Heat Treatment Distortion*, NCMS Report #0383RE97, 1997
3. D. Bammann, et al., Development of a Carburizing and Quenching Simulation Tool: A Material Model for Carburizing Steels Undergoing Phase Transformations, *2nd International Conference on Quenching and Control of Distortion*, ASM International, Materials Park, OH, 1996, p 367–375
4. Z. Li, B. Ferguson, and A. Freborg, Data Needs for Modeling Heat Treatment of Steel Parts, *Proceedings of Materials Science & Technology Conference*, 2004, p 219–226
5. B. Ferguson, Z. Li, and A. Freborg, Modeling Heat Treatment of Steel Parts, *Comput. Mater. Sci.*, 2005, **34**, p 274–281
6. V. Warke, S. Sisson, and M. Makhlouf, FEA Model for Predicting the Response of Powder Metallurgy Steel Components to Heat Treatment, *Mater. Sci. Eng., A*, 2009, **518**(1–2), p 7–15
7. B. Ferguson, A. Freborg, and Z. Li, Residual Stress and Heat Treatment—Process Design for Bending Fatigue Strength Improvement of Carburized Aerospace Gears *Proceeding of 5th International Conference on Quenching and Control Distortion*. IFHTSE Press, Berlin, 2007, p 95–104
8. A. Freborg, B. Ferguson, and Z. Li, Bending Fatigue Strength Improvement of Carburized Aerospace Gears, *Proceedings of the 23rd ASM HTS Conference*, 2005, p 186–195
9. B. Ferguson and A. Freborg, *Software to Predict Distortion of Heat Treated Components*, USAAMCOM Technical Report 02-D-46, 2002